LETTERS

Creation of a six-atom 'Schrödinger cat' state

D. Leibfried[1], E. Knill[1], S. Seidelin[1], J. Britton[1], R. B. Blakestad[1], J. Chiaverini[1]†, D. B. Hume[1], W. M. Itano[1], J. D. Jost[1], C. Langer[1], R. Ozeri[1], R. Reichle[1] & D. J. Wineland[1]

Among the classes of highly entangled states of multiple quantum systems, the so-called 'Schrödinger cat' states are particularly useful. Cat states are equal superpositions of two maximally different quantum states. They are a fundamental resource in fault-tolerant quantum computing[1–3] and quantum communication, where they can enable protocols such as open-destination teleportation[4] and secret sharing[5]. They play a role in fundamental tests of quantum mechanics[6] and enable improved signal-to-noise ratios in interferometry[7]. Cat states are very sensitive to decoherence, and as a result their preparation is challenging and can serve as a demonstration of good quantum control. Here we report the creation of cat states of up to six atomic qubits. Each qubit's state space is defined by two hyperfine ground states of a beryllium ion; the cat state corresponds to an entangled equal superposition of all the atoms in one hyperfine state and all atoms in the other hyperfine state. In our experiments, the cat states are prepared in a three-step process, irrespective of the number of entangled atoms. Together with entangled states of a different class created in Innsbruck[8], this work represents the current state-of-the-art for large entangled states in any qubit system.

One promising candidate system for scalable universal quantum information processing (QIP) consists of atomic ions that are confined in electromagnetic traps and manipulated with laser beams[9]. Most of the basic ingredients for QIP[10] have been demonstrated separately in the last few years in this system. Furthermore, some simple algorithms that could serve as primitives for larger scale QIP, including quantum error correction, teleportation, and the semiclassical quantum Fourier transform, have been implemented in the atomic-ion system.

Before large-scale QIP with atomic ions can become a reality, several challenges must be met successfully. In addition to building larger trap arrays and improving the classical control systems, it is necessary to demonstrate the ability to reliably create and maintain highly entangled states of many ions. Among such states, the so-called cat states, named after Schrödinger's cat[11], are of particular interest. Cat states are equal superpositions of two maximally different states (see below) and play a distinguished role in quantum information science. For three ion-qubits, they are also called Greenberger–Horne–Zeilinger (GHZ) states and provide a particularly clear demonstration of quantum non-locality[6]. In addition to the uses mentioned in the first paragraph, cat states can serve as a universal computation resource[12]. They are also particularly sensitive benchmarks for demonstrating good control of quantum systems[13] and the presence of entanglement. In the experiments described here, we prepared cat states of up to six ion-qubits with verifiable multi-particle entanglement.

The two states of a physical qubit are formally equivalent to the two states of a spin-1/2 magnetic moment in a magnetic field. Therefore we label our states $|\uparrow\rangle$ and $|\downarrow\rangle$ and define angular momentum operators $\tilde{S}_x, \tilde{S}_y, \tilde{S}_z$ accordingly. In particular, $\tilde{S}_z|\uparrow\rangle = \frac{1}{2}|\uparrow\rangle$ and $\tilde{S}_z|\downarrow\rangle = -\frac{1}{2}|\downarrow\rangle$ (for simplicity we set $\hbar = 1$). We define $|\overbrace{\uparrow\ldots\uparrow}^{j}, N\rangle \equiv |\uparrow\rangle_1|\uparrow\rangle_2\ldots|\uparrow\rangle_N$ and $|\overbrace{\downarrow\ldots\downarrow}^{j}, N\rangle \equiv |\downarrow\rangle_1|\downarrow\rangle_2\ldots|\downarrow\rangle_N$. In this notation, prototypical cat states of N qubits can be written as:

$$|N\,\mathrm{Cat}\rangle = \frac{1}{\sqrt{2}}(|\uparrow, N\rangle + \mathrm{e}^{i\theta}|\downarrow, N\rangle) \quad (1)$$

To generate such states we initially prepare the ions in state $|\downarrow, N\rangle$ and then apply the following unitary operation to transform the initial state into $|N\ \mathrm{Cat}\rangle$ (ref. 7):

$$U_N = \left(\exp\left[i\frac{\pi}{2}J_x\right]\exp\left[i\frac{\xi\pi}{2}J_z\right]\right)\left(\exp\left[i\frac{\pi}{2}J_z^2\right]\right)\left(\exp\left[i\frac{\pi}{2}J_x\right]\right) \quad (2)$$

The operators in the left and right pairs of parentheses represent a common rotation by angle $\frac{\pi}{2}$ of all N qubits, written in terms of the global angular momentum operators composed of the sum of the N individual spin-1/2 operators $\vec{J} = \sum_{j=1}^{N}\vec{S}_j$ (Dicke operators). The operator in the middle pair of parentheses represents a global entangling interaction that is diagonal in the measurement basis spanned by all product states of N qubits, each in either $|\uparrow\rangle$ or $|\downarrow\rangle$, and can be implemented by generalizing the phase-gate mechanism described in ref. 14 (see also below). If N is odd, $\xi = 1$; $\xi = 0$ otherwise.

Because of experimental imperfections, we need a measure to indicate how close the generated state $|\Psi_N\rangle$ is to the ideal state $|N\ \mathrm{Cat}\rangle$. The simplest measure, called the fidelity, is the square modulus of the overlap of these two states:

$$F_{N\,\mathrm{Cat}} = |\langle\Psi_N|N\,\mathrm{Cat}\rangle|^2 \quad (3)$$

To determine the fidelity of $|\Psi_N\rangle$ it is sufficient to know the probabilites $P_{\uparrow N}$, $P_{\downarrow N}$ of being in $|\uparrow, N\rangle$ or $|\downarrow, N\rangle$ and the coefficient $C_{\downarrow N;\uparrow N}$ of the $|\downarrow, N\rangle\langle\uparrow, N|$ component of the density matrix[15]

$$F_{N\,\mathrm{Cat}} = \tfrac{1}{2}(P_{\uparrow N} + P_{\downarrow N}) + |C_{\downarrow N;\uparrow N}| \geq 2|C_{\downarrow N;\uparrow N}| \quad (4)$$

where the last inequality follows from the positive semidefiniteness of density matrices.

In general, the fidelity is not sufficient as a characterization of the entanglement properties of $|\Psi_N\rangle$. For $N > 2$ there is no single measure that quantifies entanglement in all circumstances because there are many different ways in which N qubits can be entangled[16]. Consider a partition of the N qubits into disjoint subsets A and B. The qubits of A are said to be unentangled with the qubits of B if the state is a product of a state of A and of another state of B, or if the state is a mixture of such product states. In this case, non-classical correlations between A and B are absent. Conversely, the N qubits are said to exhibit genuine N-particle entanglement if there is no partition into non-empty subsets A and B for which the state is unentangled. The entanglement of two N-qubit states $|\phi\rangle$ and $|\psi\rangle$ can be compared if it is possible to obtain $|\psi\rangle$ from $|\phi\rangle$ by distributing the qubits to different parties who then apply arbitrary quantum operations and communicate classically. This means of transforming one N-qubit

[1]National Institute of Standards and Technology, 325 Broadway, Boulder, Colorado 80305, USA. †Present address: Los Alamos National Laboratory P-21, MS D454, Los Alamos, New Mexico 87545, USA.

state to another is known as 'local operations and classical communication' (LOCC)[17]. For $N > 2$ there are N-particle entangled states that cannot be transformed into each other, even if $|\psi\rangle$ need only be obtained from $|\phi\rangle$ with non-zero probability of success[18]. This implies that such states belong to different entanglement classes and that it is not possible to compare the amount of entanglement by using LOCC transformations. One of the classes with genuine N-particle entanglement is characterized by the cat states.

Establishing genuine N-particle entanglement in the experiment requires making measurements that clearly distinguish the produced state from any incompletely entangled state. One approach is based on so-called entanglement witness operators[19]. If an entanglement witness operator has a negative expectation value for a state, then that state is definitely N-particle entangled. Thus, one way to experimentally determine the presence of entanglement is to measure the expectation value of a well-chosen witness and show that it is negative with sufficient statistical significance. N-particle entanglement of cat states can be proved with a particularly simple witness operator (derived from ref. 15) based on the projector onto the ideal state $|N\,\mathrm{Cat}\rangle$:

$$W = 1 - 2|N\,\mathrm{Cat}\rangle\langle N\,\mathrm{Cat}| \tag{5}$$

The expectation value of this operator is directly related to the fidelity in equation (3):

$$\langle W\rangle = 1 - 2F_{N\,\mathrm{Cat}} \leq 1 - 4|C_{\downarrow N;\uparrow N}| \tag{6}$$

A nice feature of this entanglement measure is that if it is negative, then copies of $|\Psi_N\rangle$ can be purified by LOCC to nearly pure cat states by means of a simple and robust purification procedure[20].

Another strategy for proving N-particle entanglement is based on a 'depolarization' method. Using LOCC operations, the original density matrix can be transformed into a standard, partially depolarized form in which N-particle entanglement becomes obvious[21]. Therefore, if the depolarized state is N-particle entangled then so is the original state. The depolarized state is definitely N-particle entangled if

$$2|C_{\downarrow N;\uparrow N}| > \max_j(P_j + P_{\bar{j}}) \tag{7}$$

where P_j is the probability that state $|j\rangle$ is found upon measurement, $|j\rangle$ denotes a sequence of N ions in state $|\uparrow\rangle$ or $|\downarrow\rangle$, not all states equal, and $|\bar{j}\rangle$ corresponds to $|j\rangle$ with $\uparrow$ and $\downarrow$ interchanged. The quantities $|C_{\downarrow N;\uparrow N}|$ and $P_j + P_{\bar{j}}$ are not changed by the depolarization method. Consequently, we can obtain them directly from observations of the prepared state without actually implementing the depolarization. Inequality (7) can be satisfied even if $F < 0.5$, but the purification process to obtain nearly pure cat states with LOCC from multiple copies may no longer be simple. For our experimental six-qubit cat state (below), since $\langle W\rangle$ was found to be only slightly negative, we used the depolarization method to conclusively establish that it was six-particle entangled.

By extending methods used previously to create two- and three-qubit entangled states[7,14], we entangled up to six ions in states that approximate N-qubit cat states. We confined $^9Be^+$ ions to the axis of a linear Paul trap with axial centre-of-mass (COM) frequencies between $\omega_{\mathrm{COM}}/(2\pi) = 2.6$ MHz and $\omega_{\mathrm{COM}}/(2\pi) = 3.4$ MHz and radial COM frequencies of approximately 8 MHz (ref. 22). All N axial motional modes of the ions were cooled to the ground state by extending the method of ref. 23. We prepared the internal state of each ion in the $|F = 2, m_F = -2\rangle \equiv |\downarrow\rangle$ hyperfine ground state by optical pumping, where F and m_F are the total angular momentum and the component of the angular momentum along the quantization axis. We take $|F = 1, m_F = -1\rangle \equiv |\uparrow\rangle$ as the other qubit state. The encoding operations U_N were realized using two-photon stimulated Raman transitions uniformly applied to all ions, incorporating a phase gate G_N that is an extension of the gate described in ref. 14. The phase gate was implemented by two laser beams that uniformly illuminate all ions with a relative detuning $\omega_{\mathrm{COM}} + \delta$ with $\delta \ll \omega_{\mathrm{COM}}$, exerting a state-dependent axial optical dipole force on the ions[14]. The spacing of the ions was chosen such that the force was proportional to $\langle J_z\rangle$ (see Methods). If this dipole force is applied for a duration $t_g = 2\pi/\delta$, the motion of the COM mode is excited and de-excited in such a way that each state on which a non-zero net force acts ($\langle J_z\rangle \neq 0$) traverses a circle in phase space[14] and acquires a phase given by the area circumscribed in phase space. This area is proportional to the square of the net force and therefore to $\langle J_z^2\rangle$ for that state. In the experiment, the strength and detuning were adjusted to yield a phase of $\frac{\pi}{2}\langle J_z^2\rangle$ on each component of the wavefunction, thus realizing the third (middle) operator in equation (2). For $N = 5$ (and therefore $\xi = 1$) the left operator (up to trivial phases) was realized by an appropriate change of the final pulse: $\exp\left[i\frac{\pi}{2}J_x\right]\exp\left[i\frac{\pi}{2}J_z\right] \rightarrow \exp\left[i\frac{\pi}{2}J_y\right]$.

After creating each cat state, we determined the populations in substates with equal numbers of $|\uparrow\rangle$ components by observing state-dependent fluorescence (see Fig. 1 and Methods). The most important information on the quality of the states resides in the magnitude of coherence, $C_{\downarrow N;\uparrow N}$. A lower bound on this quantity can be extracted by executing the interferometry algorithm described in ref. 7 on the states. Here $|\Psi_N\rangle$ is 'decoded' by applying the operation $U_{N,\phi}$ to it. $U_{N,\phi}$ differs from U_N only by replacing the two J_x operations by operations $J_\phi = \cos(\phi)J_x + \sin(\phi)J_y$. Note that the effect of applying $U_{N,\phi}$ is equivalent to applying $\exp[-iJ_z\phi]U_N\exp[iJ_z\phi]$. Since this is followed by measurement, the final $\exp[-iJ_z\phi]$ has no observable effect. The first operator, $\exp[iJ_z\phi]$, is a rotation around the z-axis of the Bloch sphere and uniquely 'labels' the coherence between $|\downarrow, N\rangle$ and $|\uparrow, N\rangle$ with a phase that evolves at N times ϕ (ref. 24). The net effect is that $U_{N,\phi}$ transfers the coherence into a population difference. Ideally[7]

$$\begin{aligned}|\Psi_\phi\rangle &= U_{N,\phi}|N\,\mathrm{Cat}\rangle \\ &= -i\sin\left(\frac{N}{2}\phi\right)|\downarrow, N\rangle + i^{N+1+\xi}\cos\left(\frac{N}{2}\phi\right)|\uparrow, N\rangle\end{aligned} \tag{8}$$

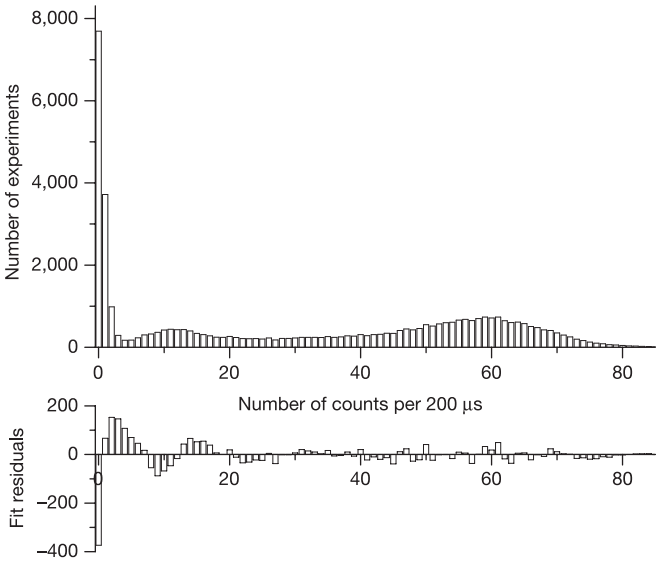

Figure 1 | Histogram and residuals of the $|6\mathrm{Cat}\rangle$. Upper plot, the experimental histogram is fitted to a sum of seven poissonian distributions with mean values corresponding to 0,1,2,…6 ions in state $|\downarrow\rangle$. The fit yields the populations $P_{|6\rangle}$, $P_{|\downarrow 6\rangle}$, and upper bounds on all other populations (see Methods). The residuals of this fit are displayed in the lower plot. The sum of all positive residuals is 1,243.6 and is forced to be equal to the sum of all negative residuals by the fitting method. The deviations of the fit from the experimental distributions are mostly due to repumping of $|\uparrow\rangle$ into fluorescing states and non-uniformity of the fluorescence detection over the ion string.

In the experiment we observed a fluorescence signal, which has a contribution that oscillates N-times sinusoidally as ϕ is ramped through 2π. This oscillation can only arise from the coherence between $|\downarrow, N\rangle$ and $|\uparrow, N\rangle$ between applications of U_N and $U_{N,\phi}$. It has a maximal amplitude $A_{\max}$ determined by the difference in the fluorescence signal with all ions in state $|\downarrow\rangle$ and the signal with all ions in state $|\uparrow\rangle$, which is achieved if all the operations are implemented perfectly. In the imperfect case, the actual amplitude of the oscillation A yields a lower bound on $|C_{\downarrow N;\uparrow N}|$ via the inequality $|C_{\downarrow N;\uparrow N}| \geq \frac{1}{2}A/A_{\max}$. Because the imperfections in $U_{N,\phi}$ match those of U_N up to the high accuracy with which pulse phases are controlled, this bound is overly pessimistic. However, it cannot be improved without introducing additional assumptions.

Figure 2 shows the fluorescence as a function of phase ϕ for 4, 5 and 6 ions obtained by the method of the previous paragraph. As the number of ions increases, the coherence is more strongly affected by several sources of imperfection. Most importantly, decoherence due to spontaneous emission increases in proportion to the number of ions and the duration of the encoding operation U_N (for six ions we estimate an 18% probability of spontaneous emission per gate). In addition, the susceptibility to magnetic field noise, which washes out the fringe contrast, grows in proportion to N (for the noise observed in our laboratory environment we estimate a dephasing time of about 150 μs for $|6\mathrm{Cat}\rangle$ that has to be compared to about 50 μs gate duration to implement U_6). As the length of the string of ions in the trap grows, rotations of all ions become less uniform owing to the approximately gaussian profile of the laser beams (for six ions, we estimate the spread in Rabi frequencies to be about 4%). Further imperfections include laser beam intensity and phase fluctuations, both of the order of 5%. In spite of these imperfections, we achieved coherences of $|C_{\downarrow 4;\uparrow 4}| \geq 0.349(2)$, $|C_{\downarrow 5;\uparrow 5}| \geq 0.264(2)$, $|C_{\downarrow 6;\uparrow 6}| \geq 0.210(2)$. The error bars in these expressions are standard deviations obtained by resampling (see Methods). For four and five ions, the coherences alone are sufficient to prove genuine four- and five-particle entanglement (equation (6)). Together with the populations from poissonian fits (see Fig. 1 and Methods) we obtain fidelities $F_{4\mathrm{Cat}} \geq 0.76(1)$, $F_{5\mathrm{Cat}} \geq 0.60(2)$ and $F_{6\mathrm{Cat}} \geq 0.509(4)$, all leading to negative values for the expectation value of witness operator W in equation (5): $\langle W_4\rangle \leq -0.51(2)$, $\langle W_5\rangle \leq -0.20(4)$ and $\langle W_6\rangle \leq -0.018(8)$. Although $\langle W_6\rangle$ is negative, it is not negative by a significant amount. To show that the state obtained has N-particle entanglement, we establish inequality (7). Although we cannot distinguish the populations P_j for different j with the same number of ions in state $|\uparrow\rangle$, we can place an upper bound on the quantities $(P_j + P_{\bar{j}})$ by using twice the maximum of the populations $P_{\downarrow 1},\ldots P_{\downarrow 5}$, where $P_{\downarrow k}$ is the probability that k ions are in the state $|\downarrow\rangle$. We obtained

$$|C_{\downarrow 6;\uparrow 6}| \geq 0.210(2) \geq \max(P_{\downarrow j}, j\epsilon\{1,2,3,4,5\}) = 0.119(9) \qquad (9)$$

so that the desired inequality is satisfied with high significance.

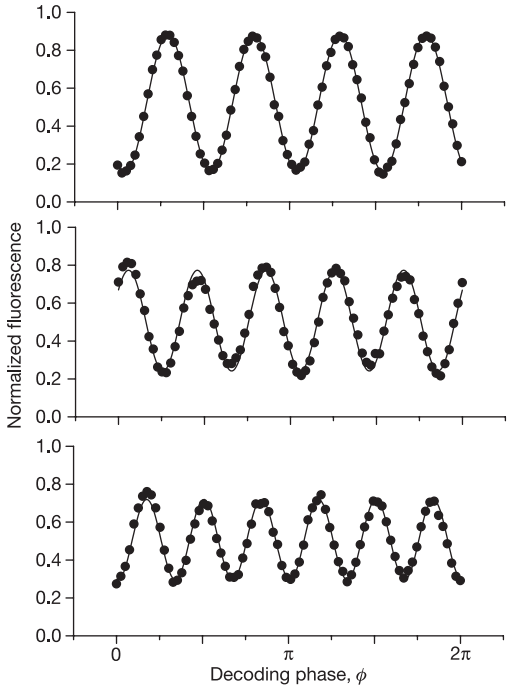

Figure 2 | Coherences of all prepared cat states. Measured traces (dots) of the normalized total ion fluorescence as the phase ϕ of the decoding gate $U_{N,\phi}$ is swept over a range of 2π for $N = 4,5,6$ (top to bottom). The fluorescence is normalized to the difference in the count rate of N ions all in state $|\downarrow\rangle$ and N ions all in $|\uparrow\rangle$. The contrast of the sinusoidal pattern with N oscillations is determined by a weighted least squares sin/cos decomposition restricted to frequencies of 0, 1,…, N. The component with frequency N is shown (solid curves). The fitted contrast gives as lower bounds for the magnitudes of the coherences in the prepared states: $|C_{\downarrow 4;\uparrow 4}| \geq 0.698(3)/2$, $|C_{\downarrow 5;\uparrow 5}| \geq 0.527(3)/2$, $|C_{\downarrow 6;\uparrow 6}| \geq 0.419(4)/2$. The differences in the starting phase arise from additional J_z rotations inherent in our implementation of the phase gates. These rotations do not affect the character or fidelity of the produced states.

It should be possible to improve state preparation in future experiments. Decoherence due to spontaneous emission may be reduced by an appropriate choice of the Raman-detuning[25] or by an entirely different choice of ion species. Magnetic field noise may be suppressed by utilizing field-independent transitions[26]. Fluctuations in beam power and phase may be actively cancelled by better feedback on the laser beams.

Cat states and the gates used to produce them are interesting in several respects. The state $|4\mathrm{Cat}\rangle$ is one of the basic building blocks for the concatenated error correcting codes used in ref. 3 to achieve fault-tolerant quantum computing with realistically noisy devices. States with a higher number of qubits could be particularly valuable for more complicated fault-tolerant encoding schemes. The direct preparation method demonstrated here could significantly reduce the overhead in such schemes. The phase gate used in the production of $|4\mathrm{Cat}\rangle$ has another interesting feature. Together with the phase gate described in ref. 14 and single-qubit rotations, it provides a universal gate set for quantum computing on a phase-decoherence-free subspace with logical qubits $\{|\downarrow\uparrow\rangle, |\uparrow\downarrow\rangle\}$ (refs 27, 28) where all gates are implemented with the same resources. Another notable feature of cat states is that they can be used to deterministically prepare Bell states of any two of the qubits by rotating and measuring the others and using the classical measurement outcomes to transform the two qubits. This feature is not shared by states such as W-states that typify some of the other entanglement classes. Bell states are the universal resource for quantum teleportation and communication between two parties. This feature is exploited in open-destination teleportation[4]. The multi-segmented trap architecture we are using should allow the distribution of entangled particles into separate locations to explore such protocols in future experiments.

Finally, spin-cat states are of particular interest in interferometry. If the contrast of the fringes in Fig. 2 were perfect, one could outperform the signal-to-noise limit of a perfect unentangled interferometer by a factor $\sqrt{N}$ and achieve the Heisenberg limit, the best possible signal-to-noise ratio within the limits of quantum uncertainty. Even with the imperfections of our experiments, all the states discussed in this Letter exhibit verified features that could not be reproduced with qubits that are not N-particle entangled, even with perfect experimental control.

METHODS

Inter-ion distance and relative phase of the dipole force. Phase gates for entangling N ions can be derived in a straightforward manner if the dipole force in the gate drive has the same phase on all ions[7]. For the arrangement of the beams in our experiment[23], the phase of the force repeats every 213 nm along the

alignment direction of the ions. The inter-ion distance is determined by the force equilibrium between mutual Coulomb repulsion of the ions and the confining force of the external trap potential, causing inter-ion distances to be unequal for $N > 3$. Nevertheless, a spacing where the dipole force has approximately the same phase for each ion can be achieved. As an example, the positions of four ions relative to the trap centre are $s(-1.437, -0.454, 0.454, 1.437)$, where $s = \sqrt[3]{e^2/(4\pi\varepsilon_0 m_{\mathrm{Be}}\omega_{\mathrm{COM}}^2)}$ is a universal scaling parameter, with e the elementary charge, ε_0 the vacuum permittivity, m_{Be} the mass of the beryllium ion and ω_{COM} the axial COM frequency. We can take advantage of the fact that the two different distances have a ratio very close to an integer ratio, 1.437/0.454 – 19/6 ≈ 0.0014, and adjust the trap frequency ω_{COM} such that all four ions are spaced close to an integer number times 213 nm. The residual error would lead to a gate infidelity of 0.004, much smaller than the imperfection produced by other sources in our experiment. Similar considerations also hold for 5 and 6 ions. The problem could be completely overcome by driving the gate on a radial COM mode instead, an option that was not available for our current laser beam set-up.

Determination of populations from state dependent fluorescence. During one detection period (duration 200 μs) we typically detect on average $\lambda_0 \approx 0.5$ counts if all ions are projected into $|\uparrow\rangle$, and about $\lambda_1 \approx 10$ additional counts for each ion in state $|\downarrow\rangle$. The parameters λ_0 and λ_1 were derived by fitting mixtures of poissonian distributions to reference photon-count histograms obtained by running many experiments for each of a small number of states including $|\downarrow, N\rangle$. We used the maximum likelihood method for fitting the histograms and parametric-bootstrap resampling for determining standard errors in inferred quantities[29]. Under the assumption that each ion fluoresces equally, the histograms should be well approximated by $E(P_{|0} \mathrm{Poiss}(\lambda_0) + P_{|1} \mathrm{Poiss}(\lambda_0 + \lambda_1) + \ldots P_{|N} \mathrm{Poiss}(\lambda_0 + N\lambda_1))$, where E is the number of experiments contributing to the histogram and Poiss(λ) is a poissonian distribution with mean λ. The parameters λ_0 and λ_1 determine the maximum possible amplitude of the phase oscillations in Fig. 2. This maximum amplitude is required for inferring a lower bound on $|C_{\downarrow N;\uparrow N}|$. The probabilities $P_{0\downarrow}, \ldots, P_{N\downarrow}$ were obtained by a maximum likelihood estimation of their values based on experimental population histograms obtained by direct observation of the prepared cat states. Up to 39,900 experiments were used to acquire these histograms. The desired witness expectations were computed according to the fits. From the populations $P_{|k}$, we determine the quantity $\frac{1}{2}(P_{\uparrow N} + P_{\downarrow N}) = \frac{1}{2}(P_{|0} + P_{|N})$, the first term in equation (4). From the remaining populations, we can find upper bounds on P_j. For example $(N = 4)$, $P_{|\uparrow\uparrow\downarrow\downarrow\rangle} \leq P_{\downarrow 2}$. Figure 1 shows the measured histogram for the six-ion cat state together with the residuals between data and the fitted distribution. The histograms and fits for four and five ions look similar. From our fitted data we find (in the order $\{P_{|0}, P_{|1}, \ldots P_{|N}\}$) $P_{4\mathrm{Cat}} = \{0.44(2), 0.079(2), 0.046(2), 0.063(2), 0.37(2)\}$, $P_{5\mathrm{Cat}} = \{0.328(6), 0.143(6), 0.044(6), 0.033(6), 0.111(6), 0.340(6)\}$, $P_{6\mathrm{Cat}} = \{0.317(9), 0.099(9), 0.061(9), 0.054(9), 0.068(9), 0.119(9), 0.282(9)\}$, for the relevant populations of the prepared cat states.

Received 27 July; accepted 20 September 2005.

1. Shor, P. W. in *Proc. 37th Symp. on the Foundations of Computer Science (FOCS)* 56–65 (IEEE Press, Los Alamitos, California, 1996).
2. Steane, A. M. & Ibinson, B. Fault-tolerant logical gate networks for css codes. Preprint at ⟨http://arxiv.org/quant-ph/0311014⟩ (2003).
3. Knill, E. Quantum computing with realistically noisy devices. *Nature* **434,** 39–44 (2005).
4. Zhao, Z. *et al.* Experimental demonstration of five-photon entanglement and open-destination teleportation. *Nature* **430,** 54–58 (2004).
5. Hillery, M., Buzek, V. & Berthiaume, A. Quantum secret sharing. *Phys. Rev. A* **59,** 1829–1834 (1999).
6. Greenberger, D. M., Horne, M., Shimony, A. & Zeilinger, A. Bell's theorem without inequalities. *Am. J. Phys.* **58,** 1131–1143 (1990).
7. Leibfried, D. *et al.* Toward Heisenberg-limited spectroscopy with multiparticle entangled states. *Science* **304,** 1476–1478 (2004).
8. Häffner, H. *et al.* Scalable multi-particle entanglement of trapped ions. *Nature* doi:10.1038/nature04279 (this issue).
9. Cirac, J. & Zoller, P. Quantum computations with cold trapped ions. *Phys. Rev. Lett.* **74,** 4091–4094 (1995).
10. DiVincenzo, D. The physical implementation of quantum computation. *Fortschr. Phys.* **48,** 771–783 (2000).
11. Schrödinger, E. Die Gegenwärtige Situation in der Quantenmechanik. *Naturwissenschaften* **23,** 807–812; 823–828; 844–849 (1935).
12. Gottesman, D. & Chuang, I. L. Demonstrating the viability of universal quantum computation using teleportation and single-qubit operations. *Nature* **402,** 390–393 (1999).
13. Knill, E., Laflamme, R., Martinez, R. & Tseng, C.-H. An algorithmic benchmark for quantum information processing. *Nature* **404,** 368–370 (2000).
14. Leibfried, D. *et al.* Experimental demonstration of a robust, high-fidelity geometric two ion-qubit phase gate. *Nature* **422,** 412–415 (2003).
15. Sackett, C. A. *et al.* Experimental entanglement of four particles. *Nature* **404,** 256–259 (2000).
16. Bennett, C. H., Popescu, S., Röhrlich, D., Smolin, J. A. & Thapliyal, A. V. Exact and asymptotic measures of multipartite pure state entanglement. *Phys. Rev. A* **63,** 012307 (2001).
17. Bennett, C. H., Bernstein, J. J., Popescu, S. & Schumacher, B. Concentrating partial entanglement by local operations. *Phys. Rev. A* **53,** 2046–2052 (1996).
18. Dür, W., Vidal, G. & Cirac, J. I. Three qubits can be entangled in two inequivalent ways. *Phys. Rev. A* **62,** 062314 (2000).
19. Lewenstein, M., Kraus, B., Cirac, J. I. & Horodecki, P. Optimization of entanglement witnesses. *Phys, Rev. A* **62,** 052310 (2000).
20. Dür, W., Aschauer, H. & Briegel, H.-J. Multiparticle entanglement purification for graph states. *Phys. Rev. Lett.* **91,** 107903 (2003).
21. Dür, W. & Cirac, J. I. Multiparticle entanglement and its experimental detection. *J. Phys. A* **34,** 6837–6850 (2001).
22. Rowe, M. A. *et al.* Transport of quantum states and separation of ions in a dual RF ion trap. *Quant. Inform. Comput.* **2,** 257–271 (2002).
23. King, B. E. *et al.* Cooling the collective motion of trapped ions to initialize a quantum register. *Phys. Rev. Lett.* **81,** 1525–1528 (1998).
24. Freeman, R. *Spin Choreography* (Oxford Univ. Press, Oxford, UK, 1998).
25. Ozeri, R. *et al.* Hyperfine coherence in the presence of spontaneous photon scattering. *Phys. Rev. Lett.* **95,** 030403 (2005).
26. Langer, C. *et al.* Long-lived qubit memory using atomic ions. *Phys. Rev. Lett.* **95,** 060502 (2005).
27. Kielpinski, D. *et al.* A decoherence-free quantum memory using trapped ions. *Science* **291,** 1013–1015 (2001).
28. Bacon, D. M. *Decoherence, Control and Symmetry in Quantum Computers*. PhD thesis, Ch. 10 Univ. California, Berkeley (2001); ⟨http://arxiv.org/quant-ph/0305025⟩ (2003).
29. Efron, B. & Tibshirani, R. J. *An Introduction to the Bootstrap* (Chapman & Hall, New York, 1993).

Acknowledgements This work was supported by the US National Security Agency (NSA) and Advanced Research and Development Activity (ARDA), by the Department of Defence Multidisciplinary University Research Initiative (MURI) programme administered by the Office of Naval Research and by NIST. We thank S. Glancy and J. Bollinger for comments on the manuscript. This paper is a contribution by the National Institute of Standards and Technology and not subject to US copyright.

Author Information Reprints and permissions information is available at npg.nature.com/reprintsandpermissions. The authors declare no competing financial interests. Correspondence and requests for materials should be addressed to D.L. (dil@boulder.nist.gov).